University of Bath

Alternative formats
If you require this document in an alternative format, please contact:
openaccess@bath.ac.uk

The Control of an Active Seat with Vehicle Suspension Preview Information

Abdulaziz Alfadhli[1]   **Jocelyn Darling**[1]   **Andrew J. Hillis**[1]

[1]Centre for Power Transmission and Motion Control, Department of Mechanical Engineering,

University of Bath, Claverton Down, Bath BA2 7AY, United Kingdom

Corresponding author:

Abdulaziz Alfadhli, Centre for Power Transmission and Motion Control, Department of

Mechanical Engineering, University of Bath, Claverton Down, Bath BA2 7AY, United

Kingdom.

Email: A.Alfadhli@bath.ac.uk

Abstract

This paper presents a novel, simple and reliable control strategy for an active seat suspension,

intended for use in a vehicle, which attenuates the harmful low frequency vertical vibration at

the driver's seat. An advantage of this strategy is that it uses measurable preview information

from the vehicle suspension. The control force is calculated from this preview information and

controller gains obtained by optimising an objective function using a genetic algorithm

approach (GA). The objective function optimises ride comfort in terms of the Seat Effective

Amplitude Transmissibility (SEAT) factor, taking into account constraints on both the

allowable seat suspension stroke and actuator force capacity. This new controller is evaluated

using both simulation and experimental tests in both the frequency and time domains. The

simulation model is based upon a linear quarter vehicle model (QvM) and a single degree of

freedom seat suspension. Experimental tests are performed using a multi-axis simulation table

(MAST) and an active seat suspension. Finally, the performance of the active seat suspension

is analysed and compared to a passive system, demonstrating significant acceleration attenuation of more than 10 dB across a broad frequency range. Consequently, this has the potential to improve ride comfort and hence reduce driver's fatigue using a reliable and cost-effective control method.

1. Introduction

Drivers of on-road and off-road vehicles are daily exposed to a wide range of different vibration levels, especially at low-frequency (1-25 Hz) in the vertical direction. It is well known that the human body is very sensitive to low-frequency whole body vibration (WBV) as this coincides with many of the human body parts' natural frequencies and, alongside discomfort, significant long-term vibration can be harmful to human health. As a result, a substantial amount of work has been undertaken to reduce whole body vibration (WBV) in vehicles, in particular, with regards to vehicle suspensions. Despite the complexity and cost of vehicle suspensions they remain generally ineffective in attenuating low-frequency WBV levels, especially in off-road vehicles. Accordingly, in off-road vehicles in particular, seat suspensions have been employed as an alternative solution as they can directly isolate the driver from transmitted vibration, are inexpensive and reliable.

There are three categories of seat suspension vibration isolation system: passive, semi-active and active. A passive seat suspension is traditionally composed of two main elements - a spring to store the vibration energy and a damper to dissipate it. The characteristics of the suspension elements are fixed and thus the isolation performance is limited, being dependent on the excitation frequency content as well as the system load, namely the driver's mass. In semi-active systems, the suspension characteristics are modulated by using adaptable suspension elements through a control strategy. The most common forms of semi-active suspension use a variable damper as a force generator and while these have a low power consumption, are inexpensive, safe and reliable, the control force is dependent upon the suspension velocity and this compromises the isolation performance. In contrast, active systems apply external forces to the system from an actuator that attenuates most of the transmitted vibration and hence the isolation performance of these systems has been shown to be superior over a wide frequency range when compared to other types of controllable suspension. However, they are expensive

and may not be reliable or fail-safe. The performance of active seat suspensions in attenuating vibration depends not only on the selection of the system hardware, such as actuators and sensors, but also on the control strategy that is used to generate the desired control force (Takács and Rohal'-Ilkiv, 2012). Consequently, many control strategies have been investigated in the past. Kawana and Shimogo (Kawana and Shimogo, 1998) conducted theoretical and experimental studies into an active seat suspension for a heavy duty truck seat that reduced the driver vertical acceleration. The active seat suspension controller was designed using optimum linear theory, based on feedback and feedforward signals, which were obtained by integrating acceleration signals.

(Choi et al., 2000) applied a skyhook controller to a semi-active seat suspension using a cylindrical magneto-rheological (MR) damper. (Huisman et al., 1993) Huismam *et al.* applied optimal control theory to design a continuous time controller for an active vehicle suspension with preview. Gu *et al.* (Gu et al., 2014) designed an H∞ controller for active seat suspensions taking into account actuator saturation and uncertainty regarding the driver's weight. However, the control was based on the assumption that the absolute velocities of the sprung and unsprung masses could be obtained through the integration of acceleration signals which is difficult to achieve accurately and reliably in practice. Kühnlein *et al.* (Kühnlein, 2007) proposed an active seat to be used in off-road vehicles using ideal seat models considering the limits in the seat suspension travel. These models were developed by generating ideal seat state values (acceleration, displacement and velocity) that minimize the SEAT factor.

A hybrid controller consisting of an adaptive feedforward filtered-x least-mean-square (FXLMS) with an H∞ feedback controller was investigated experimentally and theoretically by Wu and Chen (Wu and Chen, 2004). Even though the proposed controller succeeded in reducing vibration for a specific frequency range, it amplified vibration at other frequency ranges, which meant it was not applicable for broadband vibration typical of the random

vibration caused by road inputs. Du *et al.* (Du *et al.*, 2012) developed an active integrated seat and suspension control including a quarter-car suspension, a seat suspension, and a driver body model with 4 degrees of freedom (DOF). The authors demonstrated using simulation that the integrated seat and suspension controller reduces the driver's head acceleration more than other conventional suspensions (passive seat and suspension, active seat suspension, and active car suspension) taking into account body parameter uncertainties. However, the controller was highly complex and required signals that are difficult to obtain practically, such as the absolute velocity of the seat and the car tyre deflection. Yao et al., (Yao *et al.*, 2014) modified a robust H∞ algorithm to control an MR damper integrated with a seat suspension system taking into account parameter uncertainties and actuator constraints. In this study it was proven in simulation that the modified H∞ controller was more efficient than conventional passive and skyhook systems in reducing the vertical acceleration of the isolated mass. Similarly, a dynamic feedback H∞ algorithm with a constrained frequency range was investigated by Sun *et al.* (Sun *et al.*, 2011), taking into account the physical travel of the seat. Yagiz *et al.* (Yagiz *et al.*, 2000) designed a sliding mode controller for an active vehicle suspension using a nonlinear full vehicle model. Also Sezgin *et al.* (Sezgin *et al.*, 2016) , applied the same controller scheme to an active vehicle suspension using a quarter vehicle model and taking into account the actuator time delay.

In a recent study, Gan *et al.* (Gan *et al.*, 2015) developed an active suspension seat to attenuate periodic disturbances using an adaptive FXLMS controller. The adaptive algorithm was shown both theoretically and experimentally to attenuate vibration at the seat when excited by periodic disturbances. In (Avdagic *et al.*, 2013), a fuzzy logic controller (FLC) and an artificial neural network controller (ANNC) were studied both in simulation and experimental environments with the aim to reduce the vertical vibration of the driver seat in an off road vehicle. The first study was conducted using a FLC to modulate the stiffness of the seat suspension air spring,

whilst in the second ANNC was used to adjust the seat suspension damper. The results showed that both FLC and ANNC have the ability to reduce the vertical seat acceleration. Metered and Sika (Metered and Šika, 2014) investigated a FLC algorithm as a system controller for a semi-active MR seat suspension, with the seat suspension deflection and velocity being used as inputs. Soliman *et al.* (Soliman *et al.*, 2016) proposed a robust controller scheme that enhances the system dynamic performance considering the uncertainties in the system using a linear matrix inequality (LMI) method to force the closed-loop system poles to remain in a specific design region irrespective of system uncertainty. The controller was applied to an active vehicle suspension including the uncertainty in the passenger load and the saturation in the actuator.

Many of the Active Vibration Control (AVC) strategies found in the literature are investigated through simulation alone. In practice, many of these strategies will be difficult to implement practically. For instance, some of the strategies require online measurements of all the state variables and this increases the number of sensors and hence the cost and system complexity (Sun et al., 2011). In addition, some states are difficult to obtain, such as the absolute velocity of the seat or the driver, as in the case of the well-known classical semi-active Skyhook algorithm (Crosby and Karnopp, 1973). Many researchers have attempted to solve this problem by assuming that the system states (velocities and displacements) can be obtained by numerically integrating the measured acceleration signals. In practice, noise and signal offsets can result in inaccurate states and compromised controllers (Thong *et al.*, 2004). In other studies, it has been argued that the state variables can be estimated using an observer, but this increases the complexity of the system and also the state estimators require an accurate plant model (Fuller et al., 1996).

Preview control, which was first proposed by Bender (Bender, 1968) has been widely studied in controlling active vehicle suspensions. The idea is to provide preview information from the road prior to it reaching the vehicle tyre. There are two categories of preview control. The first

is called ''look ahead'' in which the preview information is obtained ahead of the vehicle. Then, it is fed to both active suspensions at the front and rear wheels. The second is called ''wheelbase preview'', in which preview information is acquired from the dynamic changes of the front wheels and afterwards it is used to control the active suspension at the rear wheels. Many studies (e.g. Arunachalam *et al.*, 2003) have shown that preview control potentially improves the performance of active suspensions compared to other control methods. In this paper a new control strategy for an active seat suspension is introduced which utilizes a similar idea to the preview control for a vehicle suspension. The preview information here is obtained from the vehicle suspension dynamics instead of road disturbances. The proposed controller uses realisable and low-cost preview information. It is argued that this approach compensates for actuator dynamics and time delays associated with state measurements and enhances the controllability and adaptation of the system as well as making the application practical and cost-effective.

This paper is organised as follows: Section 2 presents the proposed control strategy including the mathematical model and problem formulation. Section 3 provides a detailed explanation of the experimental test rig. An evaluation of the proposed active seat suspension based on experimental and simulation results is presented and discussed in section 4. Conclusions are presented in section 5.

2. Control strategy

In this section, the governing equations of the simulation model are obtained and the concept of the control strategy is explained. In addition, the approach used to find the optimum controller gains using a genetic optimisation algorithm is outlined.

2.1. Dynamic model

To illustrate the control method the vehicle is represented by a quarter vehicle model (QvM) with 2 DOFs. This model has been widely used in the literature as it is simple and can capture adequate information concerning the vertical motion of the vehicle (Dong *et al.*, 2010; Du *et al.*, 2003). For simplicity, the seat and the human body are assumed to be a single degree of freedom system. **Figure 1** shows the passive seat suspension integrated with a QvM model and an active actuator fixed in parallel with this suspension, in which m_{se}, m_s and m_{us} are the combined seat and driver mass, the sprung mass and the unsprung mass, respectively. The displacements of the corresponding masses in the vertical direction are x_{se}, x_s and x_{us}, respectively, while x_r is the road excitation displacement. The stiffness and damping of the seat suspension are k_{se} and c_{se}, respectively, while k_s and c_s are those of the vehicle suspension. The tyre dynamics are represented only by a stiffness k_t, as the tyre damping can be neglected. Assuming linear characteristics for both the seat suspension and vehicle suspension, the equations of motion system are derived as:

$$m_{se}\ddot{x}_{se} = -c_{se}(\dot{x}_{se} - \dot{x}_s) - k_{se}(x_{se} - x_s) + F_a \qquad (1)$$

$$m_s\ddot{x}_s = c_{se}(\dot{x}_{se} - \dot{x}_s) + k_{se}(x_{se} - x_s) - c_s(\dot{x}_s - \dot{x}_{us}) - k_s(x_s - x_{us}) - F_a \qquad (2)$$

$$m_{us}\ddot{x}_{us} = c_s(\dot{x}_s - \dot{x}_{us}) + k_s(x_s - x_{us}) - k_t(x_{us} - x_r) \qquad (3)$$

where F_a is the actuator control force.
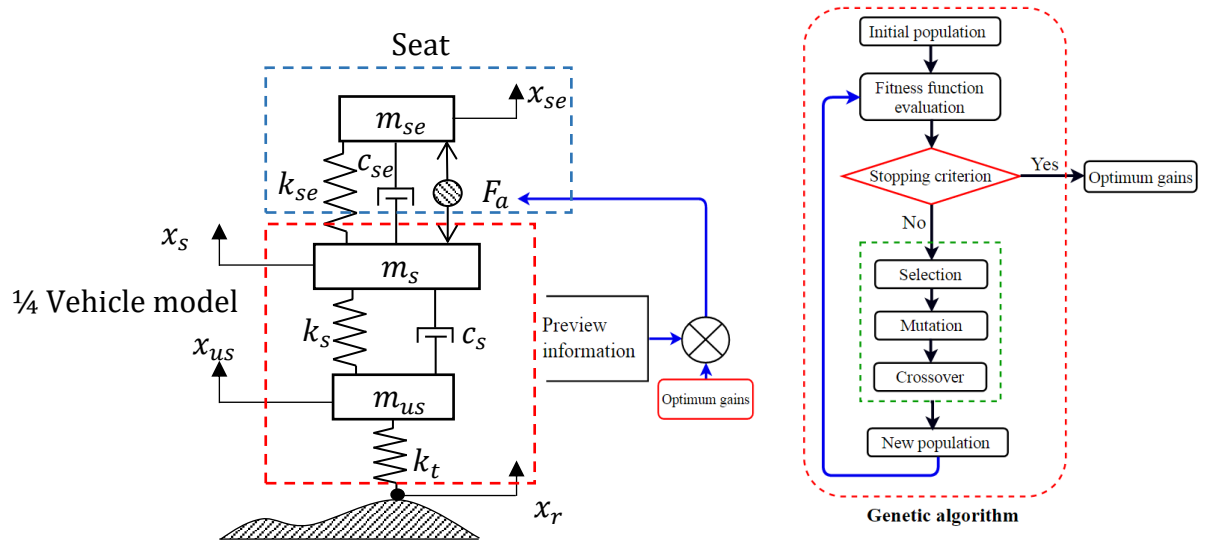
Figure 1: Seat suspension with a QvM and GA optimization algorithm

2.2. Control Force

In order to design a reliable and inexpensive active seat suspension the number of sensors and the availability of body states should be considered in the development of the control strategy. In this controller, the control force is assumed to be a linear function of preview signals from the vehicle suspension (vehicle suspension displacement and velocity) as given by:

$$F_a = q_1 \dot{x}_{rel} + q_2 x_{rel} \tag{4}$$

$$\dot{x}_{rel} = (\dot{x}_s - \dot{x}_{us}) \quad \text{and} \quad x_{rel} = (x_s - x_{us}) \tag{5}$$

where $\dot{x}_{rel}$ and x_{rel} are the relative velocity and displacement between the sprung and unsprung masses. The gains q_1 and q_2 can be determined by minimising an objective function to enhance the isolation performance of the seat suspension. This can be achieved by reducing the seat acceleration, taking into account the maximum travel of the seat suspension, this being physically limited (Baumal et al., 1998; Li et al., 2014). The ride comfort can be assessed through the Seat Effective Amplitude Transmissibility (SEAT) factor, which is defined as the ratio between the acceleration at the seat to that at the seat base (Griffin, 1996). As a result, the

SEAT factor was selected to be the objective function (Maciejewski et al., 2009), which is given by:

$$SEAT = \frac{(\ddot{x}_{se,w})_{rms}}{(\ddot{x}_{s,w})_{rms}} \qquad (6)$$

where $(\ddot{x}_{se,w})_{rms}$ is the root mean square of the seat acceleration and $(\ddot{x}_{s,w})_{rms}$ is the root mean square of the sprung mass acceleration. The subscript w means that these acceleration values are weighted according to the frequency weighting given by (ISO 2631, 1997) which considers the frequency range of 4-8 Hz in which the human body is most sensitive to vertical vibration. It is well known that minimising the seat acceleration results in an increase in the seat suspension deflection (seat stroke) which is limited (Maciejewski et al., 2009) and consequently this should be included in the optimisation problem as a constraint. In this application the maximum allowable seat stroke ($x_{se,max}$) was limited to 45 mm. In addition, the actuator force is practically limited and therefore these two factors are also included in the optimisation problem as constraints. Thus this problem is summarised as follows:

Given: A QvM with a single degree of freedom passive seat and random road input.

Find: q_1 and q_2

$$(7)$$

To minimise: $f = SEAT$

$$g(1) = (x_{se} - x_s)_{max} - (x_{se} - x_s)_{min} \leq x_{se,max}$$

Subject to:

$$g(2) = |F_a| \leq 1500 \ (N)$$

Where $g(1)$ and $g(2)$ are the seat stroke and actuator capacity force constraints, respectively. The above constrained optimisation problem can be modified to an unconstrained one using a penalty approach (Shirahatti et al., 2008), with the original objective function f being squared and multiplied by 1,000 to make it more significant to small changes in the gain values. Thus, the new objective function is given by:

$$\text{Minimize } J = 1000 * f^2 + PG \tag{8}$$

where PG is a penalty function given by:

$$PG = \begin{Bmatrix} 0 & ; \ g(1) \ and \ g(2) \leq 0 \\ 1 \times 10^{12} & ; otherwise \end{Bmatrix} \tag{9}$$

The genetic algorithm (GA) optimisation technique was selected to solve the optimization problem off-line, as shown in **Figure 1**, as it was considered a global optimisation tool and has been widely used in the literature (Baumal et al., 1998; Du et al., 2003; Gad et al., 2015). In order to solve the optimisation problem the QvM should be excited by a range of road inputs such as bump and random disturbances. These road profiles can be mathematically represented by the following formulas (Du et al., 2012):

a) **Bump road profile**

$$x_r(t) = \begin{cases} \dfrac{a}{2}\left(1 - \cos\left(\dfrac{2\pi V}{l} t\right)\right) & , 0 \leq t \leq \dfrac{l}{V} \\ 0 & , t > \dfrac{l}{V} \end{cases} \tag{10}$$

where v_0 is the forward speed of the vehicle, a and l are the height and length of the bump, respectively. In this study, it is assumed that the vehicle moves with a constant forward speed. The parameters of the bump road profile were chosen as $V = 60 \ km/h$, $a = 0.1 \ m$ and $l = 2 \ m$.

b) **Random road profile**

In order to generate a random road profile, a power spectral density (PSD) function is required. PSD depends on the measurements of the surface profile with respect to a reference plane (Tyan et al., 2009). The ISO 8608 (ISO 8608:1995) proposes an approximated formula to obtain the PSD function of the road roughness as follows:

$$\Phi(\Omega) = \Phi(\Omega_0) \left(\frac{\Omega}{\Omega_0}\right)^{-w} \tag{11}$$

Where $\Omega = \frac{2\pi}{L}$ (rad/m) is the angular spatial frequency, L is the wavelength and w is the

waviness, which has a value of 2 for most of roads. $\Phi(\Omega_0)$ is the reference PSD value for a

given road type at the reference angular spatial frequency $\Omega_0 = 1$ (rand/m). The reference

values of the PSD at $\Omega_0 = 1$ (rand/m) for different road types are given by ISO 8608 as shown

in **Table 1**. However, at low spatial frequency equation (11) tends to infinity, so that it is

modified as follows (Tyan et al., 2009):

$$\Phi(\Omega) = \begin{cases} \Phi(\Omega_0)\,\Omega_1^{-2} & \text{,for } 0 \le \Omega \le \Omega_1 \\ \Phi(\Omega_0) \left(\frac{\Omega}{\Omega_0}\right)^{-2} & \text{,for } \Omega_1 < \Omega \le \Omega_N \\ 0 & \text{,for } \Omega > \Omega_N \end{cases} \tag{12}$$

Table 1 Road roughness values at $\Omega_0 = 1$ ($\frac{rad}{m}$) (Tyan et al., 2009)

Road class	Degree of roughness $\Phi(\Omega_0)$ ($10^{-6}\ m^3$) for $\Omega_0 = 1\ rad/m$		
	Lower limit	Geometric mean	Upper limit
A (very good)	-------------------	1	2
B (good)	2	4	8
C (average)	8	16	32
D (poor)	32	64	128
E (very poor)	128	256	512

The values of Ω_1 and Ω_N are suggested by the ISO 8606 to be 0.02π (rad/m) and 6π (rad/m)

,respectively (Tyan et al., 2009) which covers a wavelength band of (0.333-100 m). When the

vehicle is traveling over a specified road segment of length L and constant velocity V, then the

random road profile as a function of a travelled path s, can be approximated using a

superposition of N ($\rightarrow \infty$) sine waves as follows:

$$x_r(s) = \sum_{n=1}^{N} A_n \, sin(\Omega_n s - \varphi_n) \qquad (13)$$

where the amplitudes A_n are given by:

$$A_n = \sqrt{\Phi(\Omega_n) \frac{\Delta\Omega}{\pi}} \qquad (14)$$

where $\Delta\Omega = \frac{\Omega_N - \Omega_1}{N-1}$ and φ_n is a random phase angle between $(0, 2\pi)$. The term Ωs in equation (13) is equivalent to:

$$\Omega s = \frac{2\pi}{\lambda} s = \frac{2\pi}{\lambda} V t = \omega t \qquad (15)$$

in which λ is the wavelength and ω (rad/sec) is the angular frequency in the time domain.

From equations (12) and (14), the road profile in the time domain is given as follows:

$$x_r(t) = \sum_{n=1}^{N} A_n \, sin(n\omega_0 t - \varphi_n) \qquad (16)$$

where $\omega_0 = V \Delta\Omega$ (rad/sec) is the fundamental temporal frequency in the time domain. Because the random road contains most of the human frequency sensitivity range and most of the road profiles are random, a random road profile is selected in the optimisation process with a very poor road roughness and a vehicle velocity of $V = 60$ km/h.

3. Experimental test rig

A test rig was developed in order to experimentally examine the performance of the active seat and control strategy. This rig consisted of two main parts, a multi-axis simulation table (MAST) and an active seat. These are described below.

3.1. Multi-axis simulation table (MAST)

The MAST is a six-degrees-of-freedom vibration simulation table which was supplied by Instron Structural Testing Systems. It provides three translation motions in Cartesian

coordinates as well as three rotations via hydraulic actuators. The MAST was used as a vibration platform for developing the active seat suspension and, by using the hardware-in-the-loop (HLP) technology, it was possible to mimic the response of a sprung mass in a simulated QvM. The hardware-in-the-loop QvM was excited by a simulated road profile which was represented mathematically as above in (eqn. 16). The resulting motion of the sprung mass was fed to the MAST to excite the active seat suspension. However, with this approach it is common to assume a perfect MAST dynamic response and often this is not the case as a result of bandwidth limitations, system friction and time delays associated with the computation of the command signals. Consequently, it is important to ensure that the MAST reasonably mimics the simulated QvM before carrying out experimental tests of the active seat, especially when the control scheme depends on the MAST's states. A block diagram of the MAST hardware-in-the-loop and the seat suspension controller is presented in **Figure 2**. In this approach, as described by the authors (Alfadhli *et al.*, 2016), the MAST was controlled to mimic the motion of the sprung mass of a QvM using the principle of HIL and the estimated dynamics of the MAST. However, the proposed controller requires two signals from the vehicle suspension to generate the active force. These signals are the sprung and unsprung mass relative displacement (x_{rel}) and velocity ($\dot{x}_{rel}$). The MAST vertical motion, which corresponds to the sprung mass motion in the QvM, was measured using a position transducer (LVDT) within the MAST hydraulic actuators, while the unsprung mass motion was estimated 'virtually' from the QvM. After obtaining the relative vehicle suspension displacement, it is differentiated to find the vehicle suspension velocity. These two signals are then fed to the control algorithm to generate the control force and can be easily measured using inexpensive commercial position transducers.
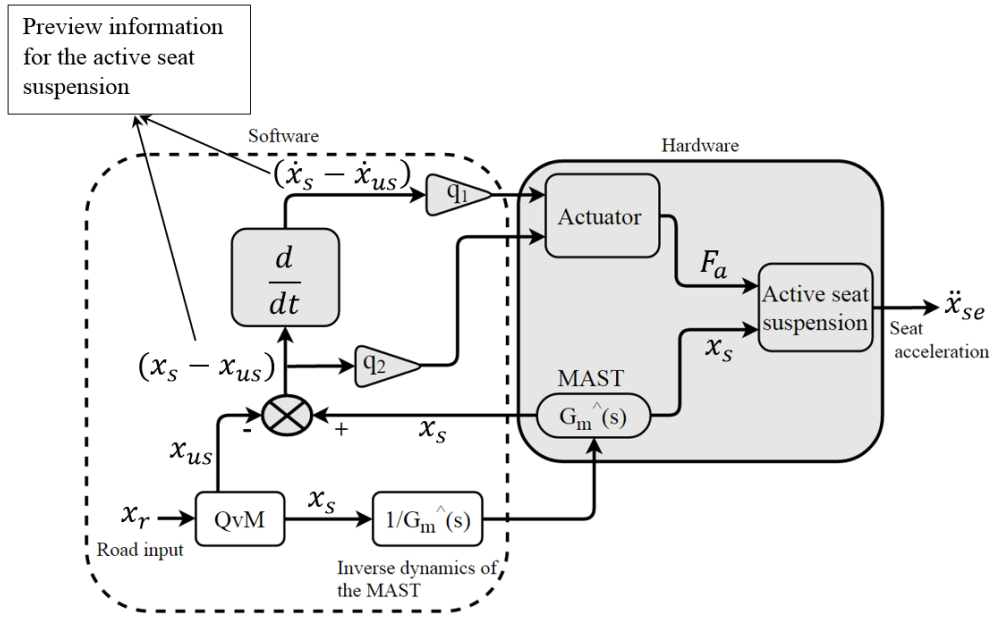
**Figure 2 Block diagram of the HIL and the proposed controller**

3.2. Active seat suspension

An active seat suspension was previously developed at the University of Bath by Gan *et al.* (Gan *et al.*, 2015), as shown in **Figure 3**. The passive suspension unit was an Elka-stage-5 bicycle shock absorber, which is comprised of a coil spring and an adjustable damper that supports the static load of the seat and driver without any need for an additional active force. This passive suspension unit is connected to the seat pan through a two-bar lever mechanism which supported the static load. Two linear rails and their corresponding carriages are used at the rear of the seat pan to allow vertical motion of the seat pan relative to the seat's frame.

The active forcing system is composed of two XTA-3806 electromagnetic linear actuators that are installed at the front and the rear of the seat pan. They each have a peak force capacity of 1.12 kN and a stroke of 30 mm with a maximum speed of 3.8 m/s. The active seat is rigidly mounted on the MAST and a test dummy with a total weight of 542 N is used to represent the dynamic response of an occupant. The seat is designed to move in heave and pitch, but only vertical motion is considered in this work so the pitch motion is rigidly constrained.

The MAST and the seat pan accelerations are measured using piezoresistive accelerometers (Entran, EGCS-D1CM-25) and the measured input and output signals are sampled at a rate of 10 kHz. An XPc data acquisition and control system is used to send signals to the MAST and to the actuators from the QvM and the control strategy, respectively. An outline of the experimental apparatus and setup are presented in **Figure 4**.
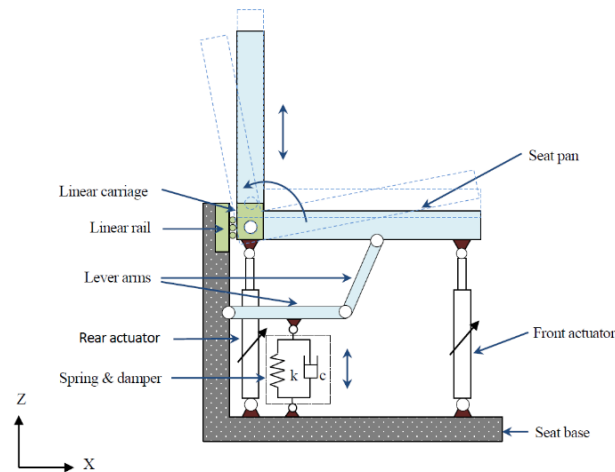
Figure 3: Schematic diagram of the active seat suspension (Gan et al., 2015)
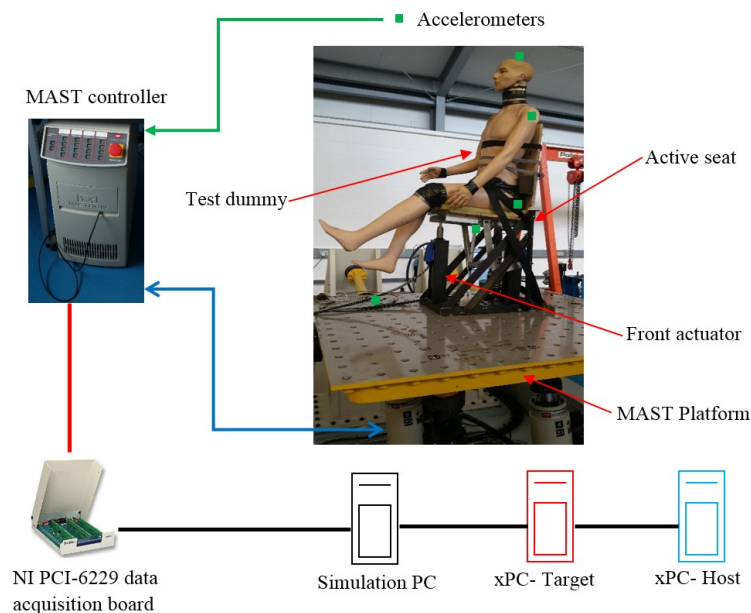

Figure 4: General experimental setup

4. Active seat evaluation

4.1. Identifying the passive seat characteristics

The vehicle and seat suspensions were modelled using Simulink and the Matlab GA optimisation tool box was used to solve the optimisation problem off-line. Many optimisation methods exist, but the GA approach is used here because it is a global optimization scheme and it is able to handle hard constraints easily, such as seat stroke and force limits. The vehicle suspension and GA parameters used in this study are given in **Table 2**. The damping and the stiffness of the simulated seat were experimentally obtained from the measured transmissibility acceleration ratio between the passive seat and the MAST, as presented in **Figure 5**.

A swept sinusoidal displacement signal with amplitude of 10.0 mm and frequency range of 0.5-18 Hz was used to excite the MAST. The resulting seat pan and MAST accelerations were measured using a sampling frequency of 10 KHz and filtered using a low pass filter with a cut-off frequency of 250 Hz. As shown in **Figure 5**, the seat and the dummy were approximated by a second order continuous transfer function system with a reasonable agreement over the frequency range of interest (< 10 Hz). This figure reveals that the (seat and dummy) system has a dominant natural frequency around 4 Hz, from which the estimated stiffness and damping of the seat were calculated as 48.75 kN/m and 1847.0 N.s/m, respectively. In addition, it shows the seat and the dummy system has additional higher order dynamics above 10 Hz owing to the multi-body nature of the dummy being excited.
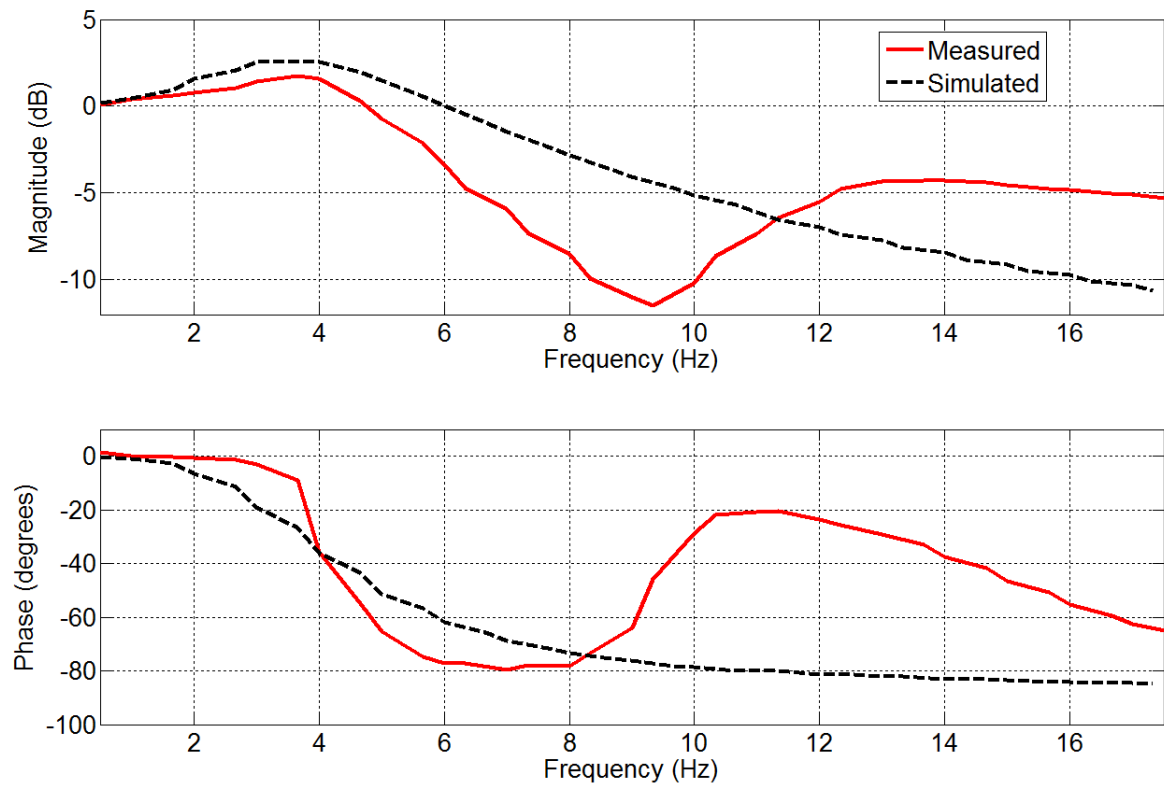
Figure 5: Measured and simulated acceleration transmissibility of the passive seat

Table 2 QvM and GA parameters

| QvM parameters		
Parameter	Value	Unit
M_s (Sprung mass)	250	Kg
M_{us} (Unsprung mass)	20	Kg
C_s (Suspension damper coefficient)	1500	N.s/m
k_s (Suspension stiffness)	10	kN/m
k_t (Tyre stiffness)	180	kN/m
GA parameters		
No. of population	40	
No. of generation	6000	
Crossover probability	0.4	
Mutation probability	0.001	

Following identification of the characteristics of the passive seat, the optimum gains q_1 and q_2 were obtained as:

$$q_1 = -64.1 \, N.s/m \quad \text{and} \quad q_2 = 5.35 \, kN/m \qquad (16)$$

Having calculated the optimum gains the proposed control strategy was applied experimentally to the active seat. The control strategy used the preview signals of the QvM suspension displacement and suspension velocity. Since the MAST was driven by a hardware-in-the-loop QvM the measured states of the MAST and the simulated states of the unsprung mass (wheel), together with the optimum gains, were used to generate the required control force from two linear actuators mounted on the active seat.

4.2. Frequency domain testing

To validate the performance of the proposed control strategy the transmissibility of the active seat was obtained over a low frequency range (0.5-18 Hz), and compared to the passive seat, as shown in **Figure 6**. It can be observed that the active system transmitted vibration at the seat is consistently less than that of the passive seat, with a maximum reduction of 10 dB, achieved at around 10 Hz. The measured frequency responses of the passive and active systems shown in **Figure 6** are also compared to those obtained from the numerical simulation, using the integrated QvM and seat models, as presented in **Figure 7**. These results prove once again the effectiveness of the proposed control strategy in reducing seat vibration both theoretically and in experimental tests. While the simulated and the experimental results for both the passive and active cases have very similar behaviours, there are differences between theory and experiment, largely caused by system non-linearities and a multi-body experimental dummy that are not included in the numerical model.
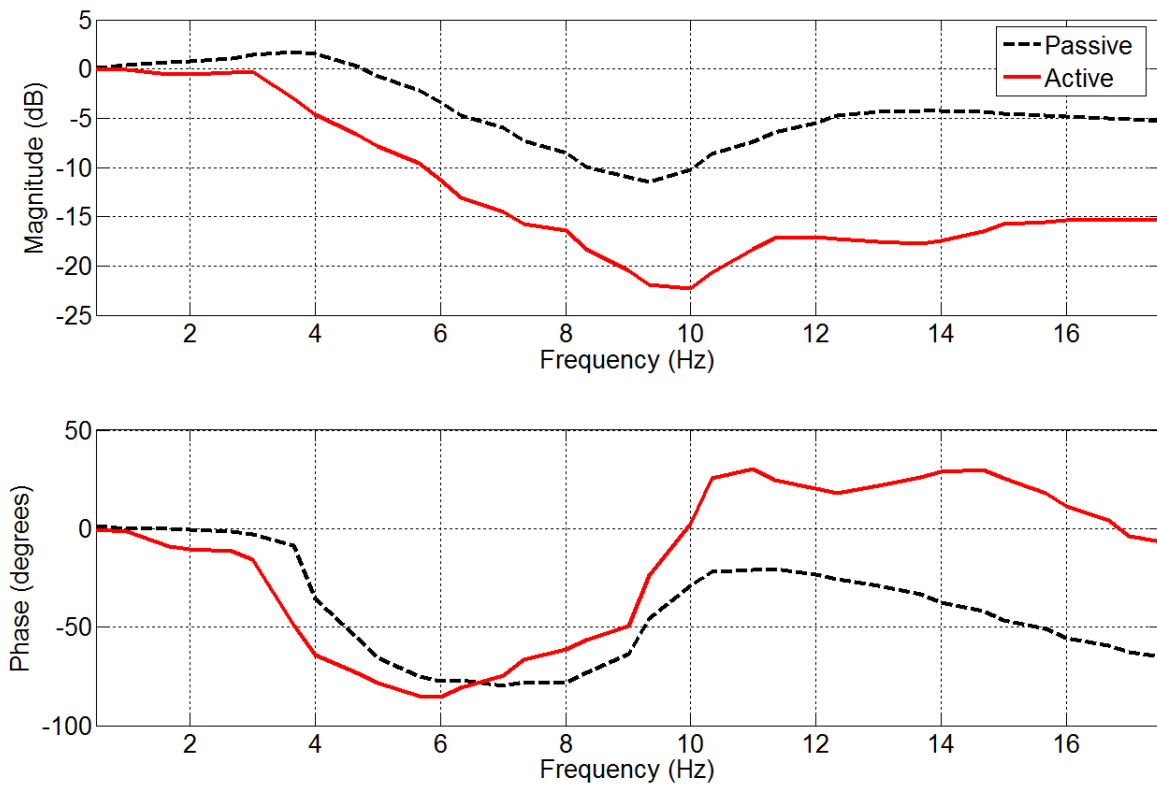
Figure 6: Measured seat acceleration transmissibilities of the passive and active systems
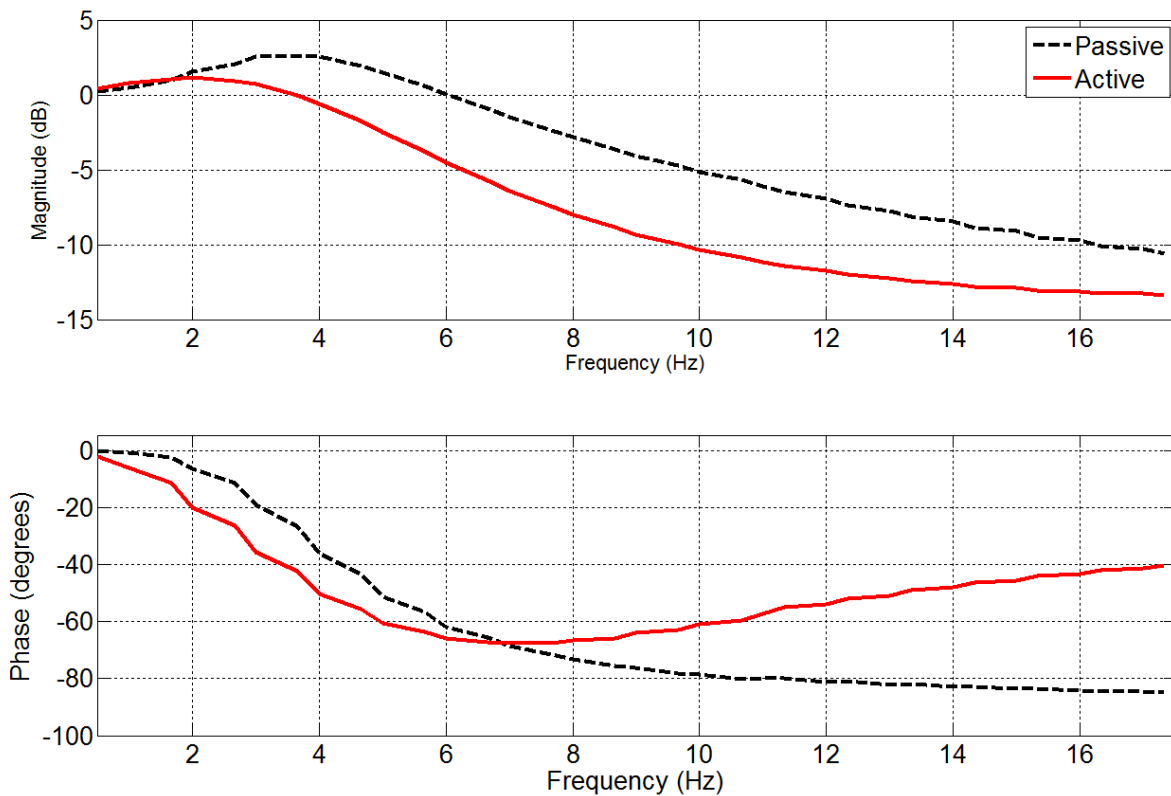
Figure 7: Simulated seat acceleration transmissibilities of the passive and active systems

4.3. Time domain

In this section the active seat with the preview control is excited by the simulated QvM, subject to random road excitation at a range of forward vehicle speeds. The assessment was carried out by comparing the passive and active SEAT factors and the maximum displacement of the active seat suspension. Furthermore, a comparison between the predicted simulation behaviour and the experimental results is made.

4.3.1. Random response

Three vehicle speeds were tested (40, 60 and 100 km/h) and due to the random nature of the road profile the simulation was carried out 100 times for each vehicle speed, with a time duration of 10 seconds. The experimental tests were repeated three times and an average taken. To avoid excessive MAST accelerations at high frequency, the reference road roughness $\Phi(\Omega_0)$ used in both the simulation and experiments was selected as $16 \times 10^{-6} \ m^3$.

The simulated and measured SEAT factors for both the passive seat and the active seat under random road excitation, are shown in **Table 3**. It can be clearly seen that the simulated and the measured SEAT factors of the active seat are lower than those of the passive system for all vehicle speeds. Moreover, the maximum percentage improvements when compared to the passive system were 32.4 % and 35.6 % for the measured and predicted systems, respectively. Once again, these results confirm the effectiveness of the active seat and the proposed controller.

The measured passive and active time responses in terms of the seat acceleration and seat suspension displacement as well as the road profiles are presented in **Figure 8**. The seat linear actuators are provided with a linear encoder having a resolution of 558 counts/mm. This was used to measure the seat suspension travel.

 It is notable that the attenuation of the vibration achieved by the active seat is greater than the passive system as it has a lower RMS seat acceleration at all vehicle speeds as given in **Table**

4. However, this improvement in the seat vibration isolation performance comes with an associated increase in the seat suspension displacement. Nevertheless, this increase does not exceed the allowable seat suspension travel.

The power spectrum densities (PSD) of the passive and active time responses are presented in **Figure 9**. At low frequencies, less than 3 Hz, the active and passive seats behave very similarly, in particular, at low and medium vehicle speeds. At higher frequencies, above 3 Hz, the active seat provides a significant reduction in the transmitted vibration PSD, indicating the effectiveness of both the controller and active system.

4.3.2. Bump response

The simulated time responses of the passive and active seat suspensions subject to a bump road profile as described by Eqn (10) at different vehicle forward speeds are given in **Figure 10**. The RMS values of both the seat acceleration and the seat suspension displacement are given in **Table 5**. It is clear from these results that the active seat reduces the seat acceleration more effectively than the passive suspension for all vehicle speeds. However, this is at the cost of increasing the seat suspension displacement. The performance of the active seat suspension at higher vehicle forward speeds is also improved as the seat suspension travel is reduced compared to that at lower vehicle speeds. These results demonstrate once again that the proposed controller can improve the ride quality of the driver, taking into account the seat suspension travel limits and actuator saturation.

Table 3 Simulated and measured SEAT factors for passive and active seat suspensions under random road excitation

| Vehicle speed (km/h)	SEAT factor					
	Passive		Active		Improvement (%)	
	Sim.	Meas.	Sim.	Meas.	Sim.	Meas.
40	79.5	93.2	50.7	73.5	36.2	21.1
60	61.9	66.7	39.5	48.8	36.1	26.8
100	57.5	59.7	37.0	40.3	35.6	32.4

Table 4 Time responses RMS values of the passive and the active seat suspensions under random road profiles

| Vehicle speed (Km/h)	Random road profile (Experimental)					
	Seat acceleration RMS (m/s²)		% Improvement	Seat suspension deflection RMS (mm)		% Increase
	Passive	Active		Passive	Active	
40	0.46	0.40	13.04	0.47	0.70	48.94
60	0.56	0.46	17.90	0.85	1.72	100.2
100	0.63	0.48	23.81	0.60	1.32	120.0

Table 5 Time responses RMS values of the passive and the active seat suspensions under bump road profiles

| Vehicle speed (Km/h)	Bump road profile (Simulated)					
	Seat acceleration RMS (m/s²)		% Improvement	Seat suspension deflection RMS (mm)		% Increase
	Passive	Active		Passive	Active	
40	1.34	1.02	31.40	1.37	1.92	40.20
60	1.37	0.92	32.90	1.22	1.53	25.40
100	1.24	0.75	39.50	0.96	1.06	10.40
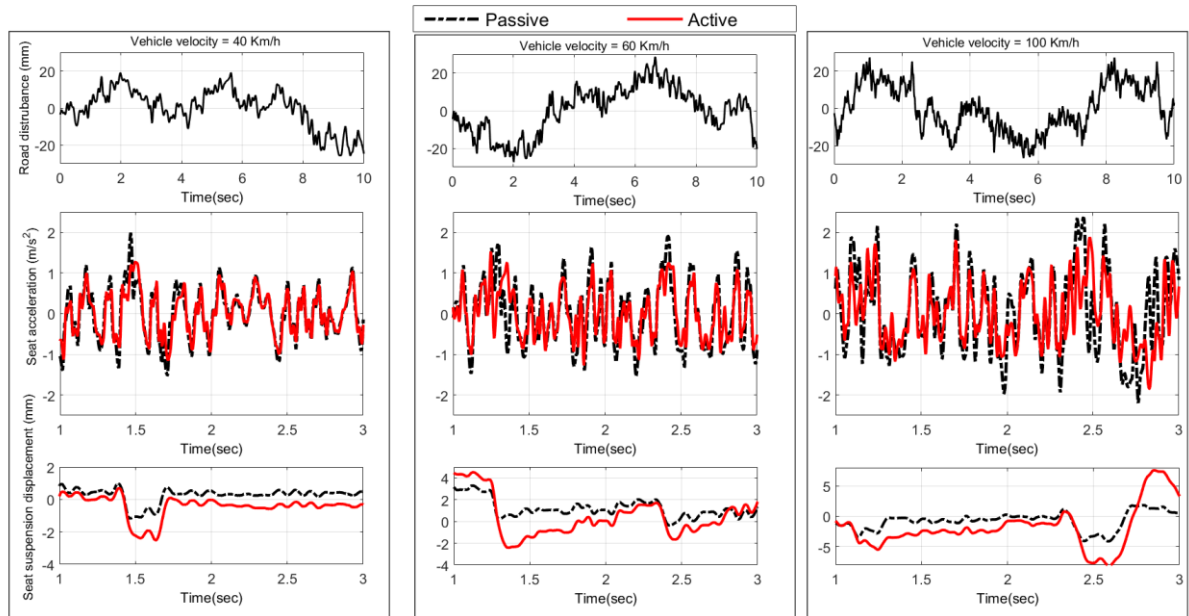
Figure 8: Measured time responses of the active and passive seats under random road excitation and different vehicle speeds
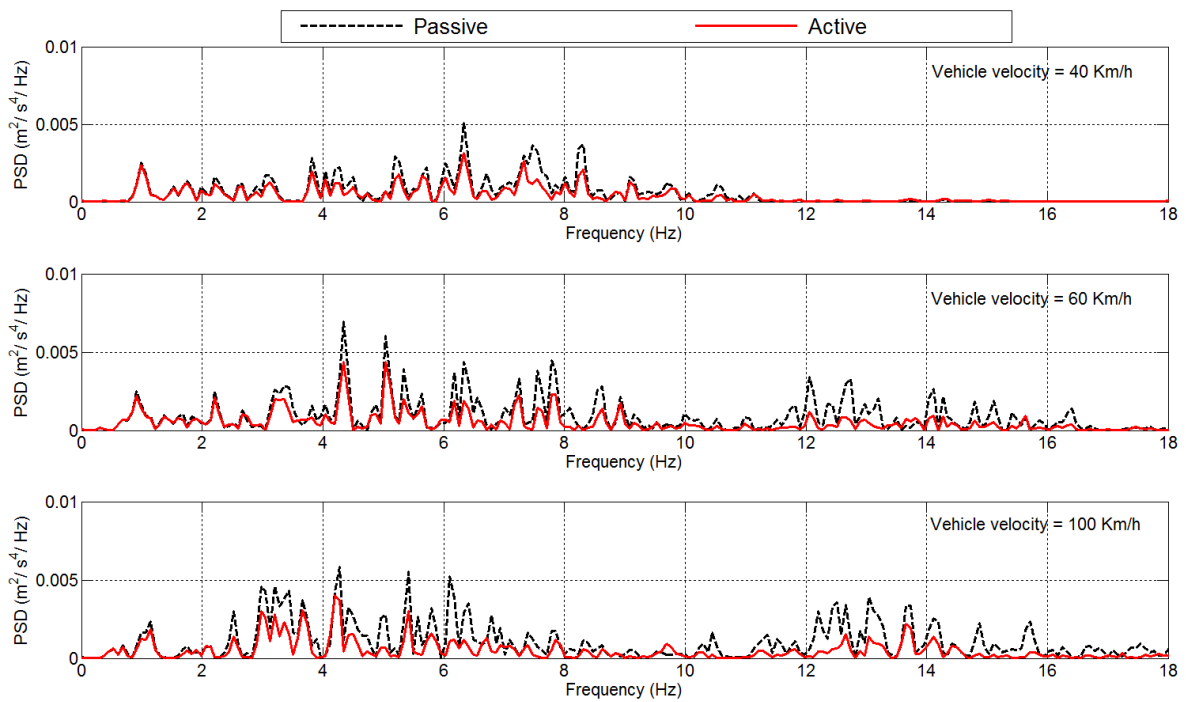
Figure 9: Measured passive and active seat acceleration power spectrum densities (PSD)
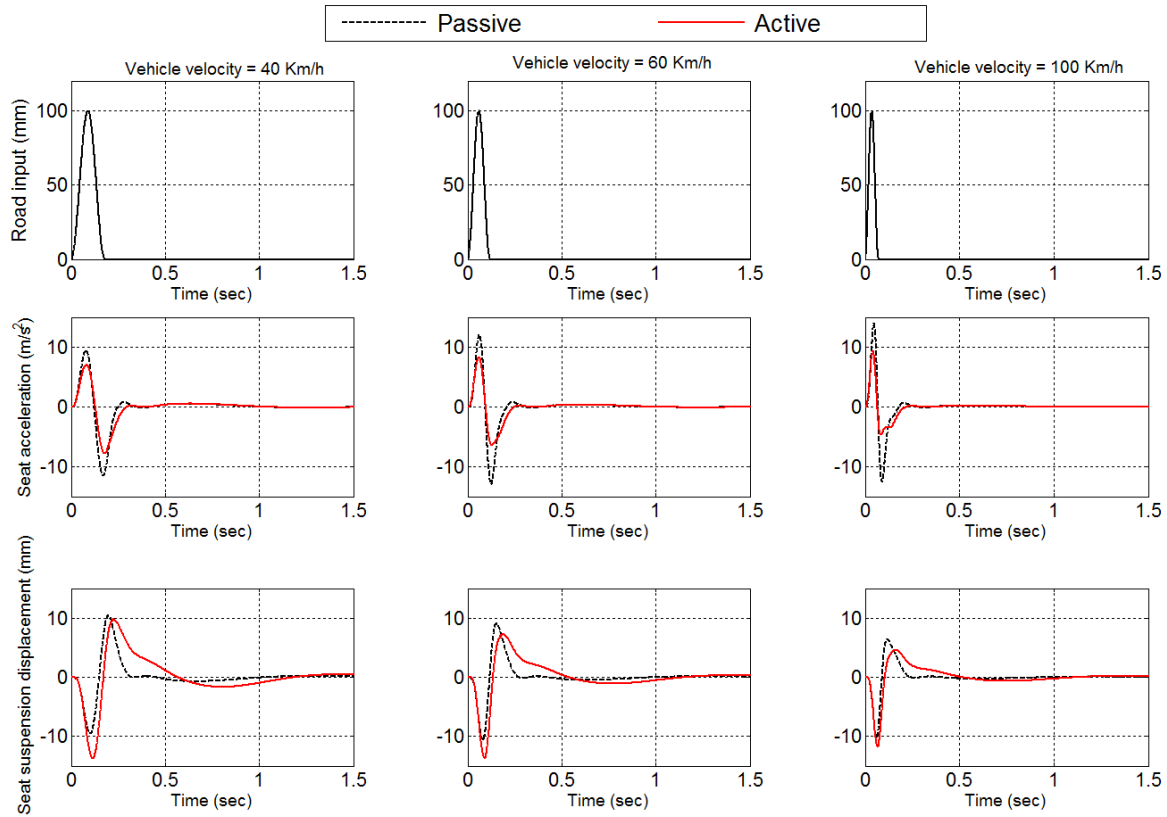
Figure 10: Simulated time responses of the active and passive seats under bump road excitation and different vehicle speeds

5. Conclusions

In this study a new, simple and cost-effective control strategy for an active seat suspension system has been developed, in order to attenuate the harmful vertical broadband vibration (1-20 Hz) transmitted to a driver as a result of road excitation. This control strategy is based on using measurable preview information from the vehicle suspension. The effectiveness of this control method has been validated through numerical simulation involving a quarter vehicle model (QvM) and laboratory experimental tests in both the frequency and time domains. Both sets of results demonstrate the effectiveness of the active controller in reducing the transmitted vibration with respect to a passive alternative, without exceeding the physical limits of either the seat suspension stroke or the actuator force capacity. Based on experimental measurements, an attenuation of more than 10 dB in the frequency domain and a 20 % improvement in the

SEAT factor have been achieved with this active seat suspension when compared with the passive alternative. Overall, this approach offers a viable, practical and cost-effective active seat controller that reduces driver's fatigue.

Acknowledgement

References

Alfadhli AEHE, Darling J and Hillis AJ (2016) Hardware-in-the-Loop (HIL) Simulation of a Quarter Vehicle Model using a Multi-axis Simulation Table (MAST). In: BATH, UK.

Arunachalam K, Jawahar PM and Tamilporai P (2003) *Active Suspension System with Preview Control-A Review*. SAE Technical Paper.

Avdagic Z, Besic I, Buza E, et al. (2013) Comparation of controllers based on Fuzzy Logic and Artificial Neural Networks for reducing vibration of the driver's seat. In: *Industrial Electronics Society, IECON 2013-39th Annual Conference of the IEEE*, IEEE, pp. 3382–3387.

Baumal AE, McPhee JJ and Calamai PH (1998) Application of genetic algorithms to the design optimization of an active vehicle suspension system. *Computer methods in applied mechanics and engineering* 163(1): 87–94.

Bender EK (1968) Optimum linear preview control with application to vehicle suspension. *Journal of Basic Engineering* 90(2): 213–221.

Choi S-B, Nam M-H and Lee B-K (2000) Vibration control of a MR seat damper for commercial vehicles. *Journal of Intelligent Material Systems and Structures* 11(12): 936–944.

Crosby MJ and Karnopp DC (1973) The active damper-a new concept for shock and vibration control. *Shock and Vibration Bulletin* 43(4): 119–133.

Dong X, Yu M, Liao C, et al. (2010) Comparative research on semi-active control strategies for magneto-rheological suspension. *Nonlinear Dynamics* 59(3): 433–453.

Du H, Lam J and Sze KY (2003) Non-fragile output feedback H∞ vehicle suspension control using genetic algorithm. *Engineering Applications of Artificial Intelligence* 16(7): 667–680.

Du H, Li W and Zhang N (2012) Integrated seat and suspension control for a quarter car with driver model. *IEEE Transactions on Vehicular Technology* 61(9): 3893–3908.

Fuller CC, Elliott S and Nelson PA (1996) *Active control of vibration*. Academic Press.

Gad S, Metered H, Bassuiny A, et al. (2015) Multi-objective genetic algorithm fractional-order PID controller for semi-active magnetorheologically damped seat suspension. *Journal of Vibration and Control*: 1077546315591620.

Gan Z, Hillis AJ and Darling J (2015) Adaptive control of an active seat for occupant vibration reduction. *Journal of Sound and Vibration* 349: 39–55.

Griffin MJ (1996) *Handbook of Human Vibration*. Elsevier.

Gu Z, Zhao Y, Gu Z, et al. (2014) Robust control of automotive active seat-suspension system subject to actuator saturation. *Journal of Dynamic Systems, Measurement and Control, Transactions of the ASME* 136(4).

Huisman RGM, Veldpaus FE, Voets HJM, et al. (1993) An optimal continuous time control strategy for active suspensions with preview. *Vehicle System Dynamics* 22(1): 43–55.

ISO 8608:1995 - *Mechanical vibration -- Road surface profiles* -- Reporting of measured data.

Kawana M and Shimogo T (1998) Active suspension of truck seat. *Shock and vibration* 5(1): 35–41.

Kühnlein A (2007) Control of an active seat for off-road vehicles using an ideal model. *Tagung Humanschwingungen, VDI Berichte 2002,VDI, Düsseldorf, Germany, pp. 553-567.*

Li P, Lam J and Cheung KC (2014) Multi-objective control for active vehicle suspension with wheelbase preview. *Journal of Sound and Vibration* 333(21): 5269–5282.

Maciejewski I, Meyer L and Krzyzynski T (2009) Modelling and multi-criteria optimisation of passive seat suspension vibro-isolating properties. *Journal of sound and Vibration* 324(3): 520–538.

Metered H and Šika Z (2014) Vibration control of a semi-active seat suspension system using magnetorheological damper. In: *Mechatronic and Embedded Systems and Applications (MESA), 2014 IEEE/ASME 10th International Conference on*, IEEE, pp. 1–7.

Sezgin A, Hacioglu Y and Yagiz N (2016) Sliding Mode Control for Active Suspension System with Actuator Delay. *World Academy of Science, Engineering and Technology, International Journal of Mechanical, Aerospace, Industrial, Mechatronic and Manufacturing Engineering* 10(8): 1356–1360.

Shirahatti A, Prasad PSS, Panzade P, et al. (2008) Optimal design of passenger car suspension for ride and road holding. *Journal of the Brazilian Society of Mechanical Sciences and Engineering* 30(1): 66–76.

Soliman HM, Benzaouia A and Yousef H (2016) Saturated robust control with regional pole placement and application to car active suspension. *Journal of Vibration and Control* 22(1): 258–269.

Sun W, Li J, Zhao Y, et al. (2011) Vibration control for active seat suspension systems via dynamic output feedback with limited frequency characteristic. *Mechatronics* 21(1): 250–260.

Takács G and Rohal'-Ilkiv B (2012) *Model Predictive Vibration Control: Efficient Constrained MPC Vibration Control for Lightly Damped Mechanical Structures*. Springer Science & Business Media.

Thong YK, Woolfson MS, Crowe JA, et al. (2004) Numerical double integration of acceleration measurements in noise. *Measurement* 36(1): 73–92.

Tyan F, Hong Y-F, Tu S-H, et al. (2009) Generation of random road profiles. *Journal of Advanced Engineering* 4(2): 1373–1378.

Wu J-D and Chen R-J (2004) Application of an active controller for reducing small-amplitude vertical vibration in a vehicle seat. *Journal of Sound and Vibration* 274(3): 939–951.

Yagiz N, Yuksek I and Sivrioglu S (2000) Robust Control of Active Suspensions for a Full Vehicle Model Using Sliding Mode Control. *JSME International Journal Series C Mechanical Systems, Machine Elements and Manufacturing* 43(2): 253–258.

Yao J, Taheri S, Tian S, et al. (2014) 1240. A novel semi-active suspension design based on decoupling skyhook control. *Journal of Vibroengineering* 16(3).

Appendix I

Notation

a	height of the bump road profile
c_s	damping coefficient of the vehicle suspension
c_{se}	damping coefficient of the seat suspension
f	optimization objective function
F_a	actuator control force
$g(1)$	seat stroke constraints
$g(2)$	actuator capacity force constraints
$\hat{G}_m$	estimated dynamics of the MAST
J	final optimization objective function
k_s	stiffness of the vehicle suspension
k_{se}	stiffness of the seat suspension
k_t	stiffness of the tyre
l	length of the bump road profile
L	length of the road segment (random road profile)
m_s	sprung mass in the QvM
m_{se}	total mass of the seat and driver
m_{us}	unsprung mass in the QvM
N	limit of the frequency range (random road profile)

PG	penalty function
q_1	optimum gain of the relative velocity of the vehicle suspension
q_2	optimum gain of the relative displacement of the vehicle suspension
$\Phi(\Omega)$	road displacement power spectral density
$\Phi(\Omega_0)$	road roughness value at the reference spatial angular frequency Ω_0
Ω	spatial angular frequency (rad/m)
λ	wavelength of the road
V	forward speed of the vehicle
x_r	vertical road excitation to the QvM
x_{rel}	relative displacement of the vehicle suspension
x_s	vertical displacement of the sprung mass
$x_{se,max}$	maximum allowable seat stroke
$x_{se,min}$	minimum allowable seat stroke
x_{se}	vertical displacement of the seat
x_{us}	vertical displacement of the usprung mass
$\left(\ddot{x}_{s,w}\right)_{rms}$	weighted root mean square of the vertical sprung mass acceleration
$\left(\ddot{x}_{se,w}\right)_{rms}$	weighted root mean square of the vertical seat acceleration
$(x_{se} - x_s)_{max}$	maximum seat stroke
$(x_{se} - x_s)_{min}$	minimum seat stroke
$\dot{x}_{rel}$	relative velocity of the vehicle suspension
$\ddot{x}_s$	vertical acceleration of the sprung mass
$\ddot{x}_{se}$	vertical acceleration of the seat
$\ddot{x}_{us}$	vertical acceleration of the usprung mass
φ_n	a random phase angle between $(0, 2\pi)$
Abbreviations	
DOFs	degrees of freedom
GA	genetic algorithm
HIP	hardware-in-the-loop simulation
MAST	multi-axis simulation table
QvM	quarter vehicle model
PSD	power spectral density function

SEAT   Seat Effective Amplitude Transmissibility factor